Proceedings of the Pakistan Academy of Sciences: A Physical and Computational Sciences 61(1): 41-49 (2024)

ISSN (Print): 2518-4245; ISSN (Online): 2518-4253
https://doi.org/10.53560/PPASA(61-1)795

Pakistan Academy of Sciences

Research Article

Geographic Object-based Image Analysis for Small Farmlands using Machine Learning Techniques on Multispectral Sentinel-2 Data

Najam Aziz[1,2], Nasru Minallah[1,2*], Muhammad Hasanat[1,2], and Muhammad Ajmal[3]

[1]Department of Computer Systems Engineering, University of Engineering and Technology, Peshawar, 25120 Pakistan
[2]National Center for Big Data & Cloud Computing (NCBC), University of Engineering and Technology Peshawar, 25120 Pakistan
[3]Department of Agricultural Engineering, University of Engineering and Technology Peshawar, 25120 Pakistan

Abstract: This study intends to classify the land cover of an area especially small farmlands using object-based image analysis (OBIA) method and evaluates the performance of a supervised classifier. Multi-spectral Sentinel-2 imagery which is freely available is used and four supervised classifiers are applied to it. The study area was divided into four major classes namely Urban, Wheat, Tobacco, and other vegetation with varying accuracy values. The imagery was first resampled to 10 m spatial resolution and then NDI45 is layer stacked to it. A widely used MRS technique is used for delineating the objects in the imagery. Finally, classification is done through four supervised classifiers *k*-Nearest Neighbour (*k*NN), Bayes classifier, Decision Tree (DT), and Random Forest (RF). The accuracy was evaluated through a confusion matrix. The results show that Sentinel-2 imagery is capable of producing thematically detailed land cover maps via the Geographic Object-Based Image Analysis (GEOBIA) approach with accuracies of *k*-NN 95%, Bayes classifier 88%, DT 81% and RF 79%.

Keywords: Classification, Geospatial Analysis, GEOBIA, Landcover, Segmentation, Sentinel-2.

1. INTRODUCTION

During the past decade, Land cover classification using remote sensing satellite imagery was a well debated topic in developed countries. Now it is also getting attention in developing countries. With the advancement in satellite technology and high-resolution imagery, the need of real-time and accurate land cover maps for the monitoring and management of natural resources, resource planning, crop yield estimation and global climate change studies, etc. has increased [1]. Remote sensing has experienced enormous advancement in recent years. With the advent of high-resolution imagery, the need for computationally efficient algorithms and object-oriented image processing is increasing. One such technique is the GEOBIA [2]. Traditionally remote sensing imagery is classified based on the pixels, a basic unit of an image. With high-resolution imagery, within pixel variability changed the concept of classification and results in OBIA [3]. Objects are a group of pixels in representative shapes and sizes having similar spectral characteristics. Unlike developed countries, where average farmland sizes are relatively high, developing countries have small structured farmland, usually less than 1 hectare [4]. With such a small size, the accurate delineation of the underlying land is an issue that is highly important for the classification of land cover [5].

Chabot *et al*. [6] utilized RF technique for tracking shallow-water aquatic plants in multi-spectral data using OBIA. They have carried out operations to monitor aquatic vegetation using the graphical software tool GIS, which may be used

Received: February 2023; Revised: December 2023; Accepted: March 2024
*Corresponding Author: Nasru Minallah <n.minallah@uetpeshawar.edu.pk>

for a very wide range of tasks. GEOBIA is utilized by Georganos *et al.* [7] for urban application. They proposed a new metric classification optimization score and concluded that it works best with rigorous feature selection and significantly reduces the processing time and storage space while producing higher classification accuracy. Rizeei *et al.* [8] also utilized this approach for Urban object extraction while using worldview-3 satellite imagery. They divided machine learning techniques in various groups of features based, object based and pixel based and concluded that feature based techniques performed better in their use case than other applied techniques. Object oriented and pixel-based approaches were also utilized in the study of Tassi and Vizzari [9]. The object-oriented method outperformed the pixel-based technique in their investigation. but with a demand of high-resolution data. This was also concluded by Blaschke *et al.* [10] and Pu *et al.* [11], that in the analysis of high-resolution images, pixel-based algorithms are unable to deliver greater accuracy.

Using GEOBIA with a digital elevation model, the study in Arctic Sweden by Stammler *et al.* [12] identified and mapped aeolian sand dunes, revealing insights into their types, orientations, and historical sediment sources. The research contributes to understanding post-glacial landscape evolution and wind patterns in this environmentally sensitive area. Another study by Islam *et al.* [13] delves into the use of machine learning algorithms, particularly random forest (RF), support vector machine (SVM), and k-nearest neighbours (*k*NN), for object-based weed and crop classification in UAV images. With a focus on a chilli crop field in Australia, the research highlights the efficiency of RF and SVM, achieving weed detection accuracies of 96% and 94%, respectively. An object-oriented image analysis work, integrating slope unit division and multi-scale segmentation, to accurately map early landslides using various features done by Gao *et al.* [14]. They tested their method in the Xianshui River basin, and their results show improved accuracy in boundary extraction. Whereas, Li *et al.* [15] integrates deep learning and object-based image analysis to accurately extract check dams, demonstrating superior performance in the Loess Plateau for effective soil conservation and management. Advancing into deep learning further, a study conducted by Ye *et al.* [16] compares Mask R-CNN deep learning with OBIA-MDTWS for cabbage plant detection in UAV images, revealing superior performance in accuracy and computing efficiency for field nursery management.

The objective of this study was to effectively identify the small farmlands cover using the geographic object-based technique from multi-spectral Sentinel-2 imagery. Similarly, another objective was to propose an efficient machine learning technique for the classification of small farmlands.

2. AREA OF INTEREST AND DATA

2.1. Area of Interest

The area of interest for this study is Yar Hussain, located in Swabi district of Khyber Pakhtunkhwa, Pakistan. It is mainly a wide arable land contributing highly to the agriculture of the province. The land cover characteristics were acquired through Sentinel-2 imagery from the Copernicus open data source and is shown in Figure 1.

2.2. Data Used

Sentinel-2 multi-spectral imagery of level-2A was acquired from the scientific data hub portal of the European Space Agency (ESA) on 26th May, 2019 [Copernicus]. One multi-spectral sensor (MSI) with 13 spectral channels is carried by the Sentinel satellite for a variety of uses [17]. The resolution

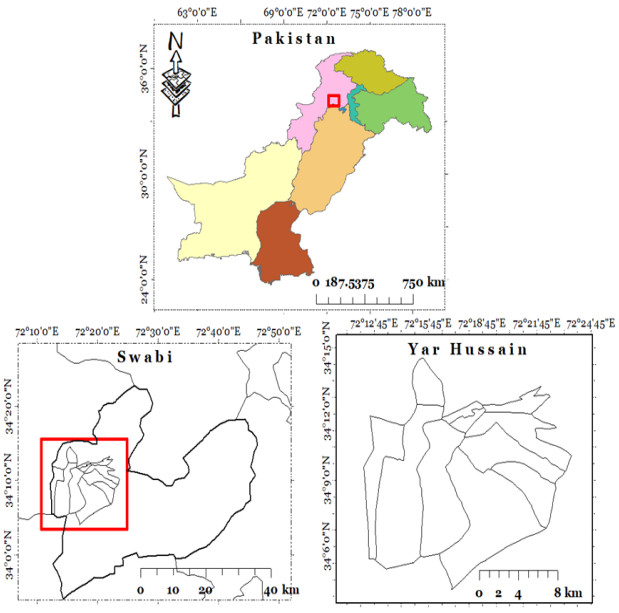

Fig. 1. Sentinel-2 imagery of the area of interest.

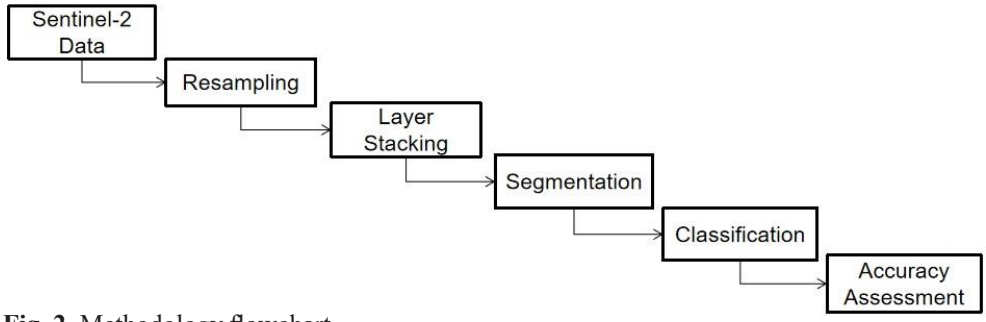

Fig. 2. Methodology flowchart.

of the channel varies between 10 and 60 m [18]. The visible (R, G, B) and near-infrared (NIR) bands are having 10 m resolution, the vegetation red edge bands (5, 6, and 7) and the short wave infrared bands (SWIR) at 20 m resolution and the rest of the bands have a resolution of 60 m [19]. Different bands of the Sentinel-2 imagery, their associated wavelengths and resolutions are shown in Table 1.

3. METHODOLOGY

A ground survey was conducted and land-cover data was collected in the study area using indigenously developed android application 'GEOsurvey'. A total of 4 classes were distinguished based on vegetated and non-vegetated areas. Further, the vegetation was divided into Wheat, Tobacco and Other vegetation classes (sugarcane, watermelon, shrubs, trees, etc.). Following that, the samples were split into training and testing samples. The classification was carried out based on training the classifier through these samples. Finally, accuracy was found through the test samples. For object-based image segmentation and classification, Definiens eCognition software was used [20]. This is the most widely used software due to its high capabilities of OBIA. The Figure 2 represent the methodology flowchart for this research work.

Table 1. Bands, their Resolution & Wavelengths of Sentinel-2.

Sentinel-2 Bands	Resolution (m)	Central Wavelength (um)
Coastal aerosol - Band 1	60	0.443
Blue - Band 2	10	0.49
Green - Band 3	10	0.56
Red - Band 4	10	0.665
Vegetation Red Edge - Band 5	20	0.705
Vegetation Red Edge - Band 6	20	0.74
Vegetation Red Edge - Band 7	20	0.783
NIR - Band 8	10	0.842
Vegetation Red Edge - Band 8A	20	0.865
Water vapor - Band 9	60	0.945
SWIR – Cirrus - Band 10	60	1.375
SWIR1 - Band 11	20	0.61
SWIR2 - Band 12	20	0.19

3.1 Pre-processing

In order to provide all the bands the same spatial resolution of 10 m, the imagery was first resampled [21]. Then NDI45 was calculated and added as an extra layer to the image [22]. The purpose of resampling was to layer stack NDI45 as an extra layer that helps in classifying vegetation. Both these tasks are carried out in the SNAP (Sentinel Application Platform). The layer stacked imagery was exported to eCognition for further processing. Training and testing samples were imported to eCognition as thematic layer. A rule-set is developed whereby all the processes take place according to that rule set.

3.2 Segmentation

In OBIA, image was converted to segments/objects and then these objects were used as the basic unit of imagery for classification [23]. Meaningful segmentation is the most important issue in the OBIA. There are many segmentation algorithms provided in Definiens eCognition that deals with object creation [24]. In this research, multi-resolution segmentation (MRS) which is the most widely used segmentation algorithm has been applied.

Through an iterative algorithm, the MRS assembles objects by grouping them, starting from individual pixels and continuing until a specified threshold, indicating the upper limit of object variance, is reached. The MRS is

controlled by three main factors including Scale, Shape and Compactness. These factors affect the overall segmentation process. Scale parameter or homogeneity criteria is user-defined threshold that establishes the highest permissible heterogeneity for the resulting segments. It controls the amount of spectral variation within objects. The process of segmentation terminates when a small increase in homogeneity exceeds the user-defined scale parameter as a threshold. Hence higher Scale Parameter (SP) value will result in bigger objects and vice versa. The SP considers the shape and colour of the objects while segmenting the image. If Shape is 0, this means that only colour is considered during segmentation, else if shape > 0, the colour as well as shape affects the segmentation process. The higher the value of the shape, the higher the weight shape is having in the resulting segments while producing fewer fractal boundaries between objects.

In this study, different levels of segmentation were carried out to achieve the best possible segments that describe the actual surface conditions of the image. The classification has been applied to the segmented imagery with a SP of 20, as it achieved the formation of fine objects. Figure 3 shows the segmented image with a SP value of 20, shape and compactness value of 0.9 and 0.5, respectively. The MRS also allows to assign different weights to spectral bands based on their importance in the underlying scenario. The weight of 5 is used for NDI45, NIR, and green bands. While RE1, RE2, RE3, and RE4 were given a weight of 2. Band 1 and band 10 were set to zero as these don't have significant contributions to this study.

3.3 Assigning Training Samples

Training samples collected during the ground survey were divided into training and testing sets and imported as a thematic layer into eCognition. The classes were assigned through these thematic layers. Eventually, the assigned objects were converted to sample objects and used for classification.

3.4 Classification

3.4.1. k – Nearest Neighbor (kNN)

The *k*-NN technique is the most straightforward machine learning algorithm. It is utilized for the classification of objects using nearby training examples in the feature space [25]. Based on the class properties of its *k* closest neighbours, an object is categorized using this approach. The ideal value of *k* for the training sample set was determined by examining various values of *k* [26]. After examination, it was found that for $k = 3$, it gives optimal results. K-NN uses the Euclidean distance between two points. When the feature space has m dimensions, two locations A and B are represented by feature vectors A = (x1, x2,..., xm) and B = (y1, y2,..., ym). Then the following formula is used to determine the separation between A and B:

$$d(A, B) = \sqrt{\sum_{i=1}^{m}(x_i - y_i)^2} \quad (1)$$

3.4.2. Bayes classifier

The Bayes classifier is based on the Bayes theorem of Bayesian statistics, which is a straightforward probabilistic classifier with solid independent

Fig. 3. MRS Segmented imagery with a magnified view.

assumptions. The presence (or absence) of one feature of a class is assumed to be independent of the presence (or absence) of any other feature(s). It is presumptive that the existence (or absence) of one feature of a class is unrelated to the presence (or absence) of any other feature [27]. It assumes that each feature works on its own to increase the likelihood that an unknown object belongs to a certain class. The Bayes classifier has the advantage of using less training data to determine the classification-related parameters (variable means and variances). Assuming independent variables, only the variances of the variables for each class need to be calculated, not the entire covariance matrix.

3.4.3. Decision tree

The DT is a machine learning algorithm that predicts the value of the target variable based on a number of input features. In OBIA, it predicts an unknown object based on training samples which have known classes [28]. As the MRS has various parameters for thresholding, the Decision Tree is a potential approach for modelling the problem.

3.4.4. Random forest

The RF is an ensemble learning technique that creates numerous DTs that are randomly produced and then aggregated to compute a classification [29]. It combines weaker, decorrelated classification trees and aggregate them for computing classification. When classifying land cover classes, the RF is proven to be reliable and effective algorithm [30]. Figure. 4. Shows the land cover of the study area classified by the KNN, Bayes, DT and RF classifier.

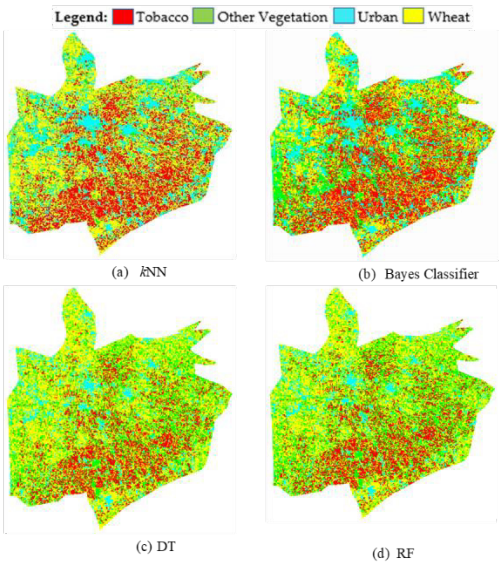

Fig. 4. Classified land cover of the study area using (a) kNN (b) Bayes (c) Decision Tree, and (d) RF Classifier.

4. RESULTS AND DISCUSSION

This study's goal was to assess how well the OBIA technique performed when used with Sentinel-2 data in areas having small farmland and sparse agriculture. The image objects delineated by the MRS were further classified by supervised classifier *k*-NN, Bayes classifier, DT and RF. The accuracy of these classifiers was assessed using a confusion matrix and is shown in Table 2, Table 3, Table 4, and Table 5, respectively. It was found that the *k*NN performed the best with overall accuracy (OA) of 95% and kappa Coefficient (KIA) of 0.91, followed by the Bayesian classifier with OA of 88% and KIA value of 0.82. The DT and RF have the OA of 81% and 79%, with KIA values of 0.72 and 0.70, respectively. The overall accuracy for various classifiers is calculated from the confusion matrix using the following mathematical formulation:

$$\text{Overall Accuracy} = \text{Correctly classified pixel/ Total number of classified pixels} \quad (2)$$

Below is a detailed discussion of the individual tables that represent the performance of the models. The k-Nearest Neighbors (kNN) classifier demonstrates strong performance across all land cover classes (Table 2). Notably, it achieves high user accuracies for Urban (97%), Wheat (92%), Other Vegetation (91%), and Tobacco (96%). The overall accuracy stands at an impressive 95%, indicating the model's effectiveness in classifying the samples. The Kappa Index of Agreement (KIA) further supports the robustness of the classifier, registering at 0.917, signifying substantial agreement beyond chance. The Bayes classifier exhibits commendable accuracy in classifying Urban (93%), Wheat (92%), and Tobacco (95%) land cover types (Table 3). However, it faces challenges in accurately categorizing Other Vegetation, with a notably lower accuracy of 42%. The overall accuracy is 88%, and the Kappa Index of Agreement (KIA) is 0.825, suggesting a substantial level of agreement. Despite the lower accuracy in one category, the Bayes classifier demonstrates competitive performance across the majority of land cover classes.

The Decision Tree classifier excels in accurately classifying Urban (93%) and Tobacco (98%) land cover types (Table 4). However, it struggles with Wheat (82%) and Other Vegetation (27%), indicating limitations in these specific classifications. The overall accuracy is 81%, with a Kappa Index of Agreement (KIA) of 0.725, signifying substantial agreement. While the model performs well in certain categories, improvements are needed for more balanced accuracy across all land cover types. Similar to the Decision Tree, the Random Forest classifier demonstrates high accuracy for Urban (93%) and Tobacco (98%) land cover types (Table 5). However, it faces challenges in accurately classifying Wheat (82%) and Other Vegetation (25%). The overall accuracy is 79%, with a Kappa Index of Agreement (KIA) of 0.705, indicating substantial agreement. While the model excels in specific categories, efforts should be directed towards improving accuracy for the challenging classes, such as Other Vegetation.

While comparing the results, all the classifiers were observed to perform more effectively. for urban, wheat and tobacco classes and is evident from the producer and user accuracies of these classes for all the applied classifiers. But the 'other vegetation' class is usually confused and misclassified with other classes in all the classifiers. For example, in KNN classification, the 'Other vegetation' class has a producer accuracy of 65% while user accuracy is 91%. This means that although 65% of the reference 'other vegetation' areas have been correctly classified as other vegetation, but 91% of the areas identified as "other vegetation" in the classification are actually other vegetation. The producer and user accuracies of other vegetation in Bayesian are 73% and 42%, in DT 80% and 27%, and in RF are 81% and 25%, respectively. This misclassification of other vegetation class in all the classifiers may be because of the overlap of some of the other vegetation areas with tobacco class due to its similarity, while the vegetation areas which are not fully grown and have more exposed barren land are confused with the wheat class as the wheat was in reaped stages.

Finally, the classification results also show that for some areas in the imagery, especially around borders, the pixels are not correctly categorized. The reason might be the extracted objects which are having different scale parameters. The similarity

Table 2. Confusion Matrix for classification using *k*NN.

User Class\Sample	Urban	Wheat	Other Vegetation	Tobacco	Sum	User Accuracy
Urban	315	4	4	2	325	97%
Wheat	8	488	17	17	530	92%
Other Vegetation	1	5	71	1	78	91%
Tobacco	2	22	17	886	927	96%
Sum	326	519	109	906		
Producer Accuracy	97%	94%	65%	98%		
Overall Accuracy	95%					
KIA	0.917					

Table 3. Confusion Matrix for classification using Bayes Classifier.

User Class\Sample	Urban	Wheat	Other vegetation	Tobacco	Sum	User Accuracy
Urban	306	13	3	7	329	93%
Wheat	7	409	18	14	448	92%
Other Vegetation	10	64	79	34	187	42%
Tobacco	3	33	9	851	896	95%
Sum	326	519	109	906		
Producer Accuracy	94%	79%	73%	94%		
Overall Accuracy	88%					
KIA	0.825					

Table 4. Confusion Matrix for classification using DT.

User Class\Sample	Urban	Wheat	Other vegetation	Tobacco	Sum	User Accuracy
Urban	273	18	1	1	293	93%
Wheat	44	400	18	29	491	82%
Other vegetation	9	93	87	129	318	27%
Tobacco	0	8	3	747	758	98%
Sum	326	519	109	906		
Producer	84%	77%	80%	83%		
Overall Accuracy	81%					
KIA	0.725					

Table 5. Confusion Matrix for classification using RF.

User Class\Sample	Urban	Wheat	Other vegetation	Tobacco	Sum	User Accuracy
Urban	270	17	1	1	289	93%
Wheat	46	371	17	21	455	82%
Other vegetation	10	120	88	134	352	25%
Tobacco	0	11	3	750	764	98%
Sum	326	519	109	906		
Producer	83%	72%	81%	83%		
Overall Accuracy	79%					
KIA	0.705					

between the spectral signature of some of the classes, such as wheat, immature other vegetation and urban structures makes them highly difficult to distinguish while working with the supervised classification method. It is expected that the introduction of more features like textural or spectral to the classifying algorithm may improve its quality.

5. CONCLUSIONS

This study significantly contributes to land cover mapping in small farmlands by utilizing Sentinel-2 imagery and GEOBIA, achieving a remarkable 95% accuracy with the *k*-NN classifier. Emphasizing the importance of finer object segmentation and accurate ground truth data, the research provides valuable insights into the successful application of these techniques in small agricultural landscapes. The study's findings offer a practical and effective approach for creating comprehensive thematic maps, showcasing the potential of GEOBIA on open-source satellite imagery for detailed land cover assessment.

6. CONFLICT OF INTEREST

The authors declare no conflict of interest.

7. REFERENCES

1. P.T. Noi, and M. Kappas. Comparison of random forest, k-nearest neighbor, and support vector machine classifiers for land cover classification using Sentinel-2 imagery. *Sensors* 18(1): 18 (2018).
2. X. Zhang, G. Chen, W. Wang, Q. Wang, and F. Dai. Object-based land-cover supervised classification for very-high-resolution UAV images using stacked denoising autoencoders. *IEEE Journal of Selected Topics in Applied Earth Observations and Remote Sensing* 10(7): 3373-3385 (2017).
3. X. Zhang, Q. Wang, G. Chen, F. Dai, K. Zhu, Y. Gong, and Y. Xie. An object-based supervised classification framework for very-high-resolution remote sensing images using convolutional neural networks. *Remote Sensing Letters* 9(4): 373-382 (2018).
4. J. Böhler, M. Schaepman, and M. Kneubühler. Crop classification in a heterogeneous arable landscape using uncalibrated UAV data. *Remote Sensing* 10(8): 1282 (2018).
5. B. Watkins, and A. Van Niekerk. A comparison of object-based image analysis approaches for field boundary delineation using multi-temporal Sentinel-2 imagery. *Computers and Electronics in Agriculture* 158: 294-302 (2019).
6. D. Chabot, C. Dillon, A. Shemrock, N. Weissflog, and E. P. Sager. An object-based image analysis workflow for monitoring shallow-water aquatic

vegetation in multispectral drone imagery. *ISPRS International Journal of Geo-Information* 7(8): 294 (2018).
7. S. Georganos, T. Grippa, S. Vanhuysse, M. Lennert, M. Shimoni, S. Kalogirou, and E. Wolff. Less is more: Optimizing classification performance through feature selection in a very-high-resolution remote sensing object-based urban application. *GIScience & Remote Sensing* 55(2): 221-242 (2018).
8. H.M. Rizeei, B. Pradhan, and M.A. Saharkhiz. Urban object extraction using Dempster Shafer feature-based image analysis from worldview-3 satellite imagery. *International Journal of Remote Sensing* 40(3): 1092-1119 (2019).
9. A. Tassi, and M. Vizzari. Object-oriented lulc classification in google earth engine combining snic, glcm, and machine learning algorithms. *Remote Sensing* 12(22): 3776 (2020).
10. T. Blaschke, C. Burnett, and A. Pekkarinen. Image segmentation methods for object-based analysis and classification. In: *Remote sensing image analysis: Including the spatial domain*, F.D. Meer and S. de Jong (Eds*.) Springer, Dordrecht* pp. 211-236 (2004).
11. R. Pu, S. Landry, and Q. Yu. Object-based urban detailed land cover classification with high spatial resolution IKONOS imagery. *International Journal of Remote Sensing* 32(12): 3285-3308 (2011).
12. M. Stammler, T. Stevens, and D. Hölbling. Geographic object-based image analysis (GEOBIA) of the distribution and characteristics of aeolian sand dunes in Arctic Sweden. *Permafrost and Periglacial Processes* 34(1): 22-36 (2023).
13. N. Islam, M.M. Rashid, S. Wibowo, C.Y. Xu, A. Morshed, S.A. Wasimi, and S.M. Rahman. Early weed detection using image processing and machine learning techniques in an Australian chilli farm. *Agriculture* 11(5): 387 (2021).
14. H. Gao, L. He, Z.W. He, and W.Q. Bai. Early landslide mapping with slope units division and multi-scale object-based image analysis-A case study in the Xianshui river basin of Sichuan, China. *Journal of Mountain Science* 19(6): 1618-1632 (2022).
15. S. Li, L. Xiong, G. Hu, W. Dang, G. Tang, and J. Strobl. Extracting check dam areas from high-resolution imagery based on the integration of object-based image analysis and deep learning. *Land Degradation & Development* 32(7): 2303-2317 (2021).
16. Z. Ye, K. Yang, Y. Lin, S. Guo, Y. Sun, X. Chen, and H. Zhang. A comparison between Pixel-based deep learning and Object-based image analysis (OBIA) for individual detection of cabbage plants based on UAV Visible-light images. *Computers and Electronics in Agriculture* 209: 107822 (2023).
17. G. Kaplan, and U. Avdan. Object-based water body extraction model using Sentinel-2 satellite imagery. *European Journal of Remote Sensing* 50(1): 137-143 (2017).
18. F.B. Balcik, G. Senel, and C. Goksel. Greenhouse Mapping using Object Based Classification and Sentinel-2 Satellite Imagery. *8th International Conference on Agro-Geoinformatics (Agro-Geoinformatics)* IEEE, pp. 1-5 (2019).
19. A. Novelli, M.A. Aguilar, A. Nemmaoui, F.J. Aguilar, and E. Tarantino. Performance evaluation of object based greenhouse detection from Sentinel-2 MSI and Landsat 8 OLI data: A case study from Almería (Spain). *International Journal of Applied Earth Observation and Geoinformation* 52: 403-411 (2016).
20. T. Blaschke. Object based image analysis for remote sensing. *ISPRS journal of photogrammetry and remote sensing* 65(1): 2-16 (2010).
21. J.P. Arroyo-Mora, M. Kalacska, R. Soffer, G. Ifimov, G. Leblanc, E.S. Schaaf, and O. Lucanus. Evaluation of phenospectral dynamics with Sentinel-2A using a bottom-up approach in a northern ombrotrophic peatland. *Remote sensing of environment* 216: 544-560 (2018).
22. F. Di Palma, F. Amato, G. Nolè, F. Martellozzo, and B. Murgante. A SMAP supervised classification of landsat images for urban sprawl evaluation. *ISPRS International Journal of Geo-Information* 5(7): 109 (2016).
23. E. Hussain, and J. Shan. Object-based urban land cover classification using rule inheritance over very high-resolution multisensor and multitemporal data. *GIScience and Remote Sensing* 53(2): 164-182 (2016).
24. S.A.P. Bentir, A.K.D. Balan, A.H. Ballado, and J.B. Lazaro. Optimization of object—based image segmentation in classifying water region. *In 3rd International Conference on Control and Robotics Engineering (ICCRE)*. IEEE, pp. 249-253 (2018).
25. M. Rana, and S. Kharel. Feature Extraction for Urban and Agricultural Domains Using Ecognition Developer. *International Archives of the Photogrammetry, Remote Sensing and Spatial Information Sciences* 42: 609-615 (2019).
26. C. Munyati. Optimising multiresolution segmentation: delineating savannah vegetation boundaries in the Kruger National Park, South Africa, using Sentinel 2 MSI imagery. *International Journal of Remote Sensing* 39(18): 5997-6019 (2018).
27. J. Fethers. Remote Sensing of Eelgrass using Object Based Image Analysis and Sentinel-2 Imagery. M.Sc. Thesis. *Aalborg University, Copenhagen, Denmark* (2018).
28. L.A. Ruiz, J.A. Recio, P. Crespo-Peremarch, and M. Sapena. An object-based approach for mapping forest structural types based on low-density LiDAR and multispectral imagery. *Geocarto International*

33(5): 443-457 (2018).
29. V. Lebourgeois, S. Dupuy, E. Vintrou, M. Ameline,S. Butler, and A. Bégué. A combined random forest and OBIA classification scheme for mapping smallholder agriculture at different nomenclature levels using multisource data (simulated Sentinel-2 time series, VHRS and DEM). *Remote Sensing* 9(3): 259 (2017).
30. R.L. Lawrence, S.D. Wood, and R.L. Sheley. Mapping invasive plants using hyperspectral imagery and Breiman Cutler classifications (Random Forest). *Remote Sensing of Environment* 100(3): 356-362 (2006).